Cell, Vol. 111, 41–50, October 4, 2002, Copyright ©2002 by Cell Press

The Circadian Gene *Period2* Plays an Important Role in Tumor Suppression and DNA Damage Response In Vivo

Loning Fu,[1] Helene Pelicano,[2] Jinsong Liu,[3] Peng Huang,[2] and Cheng Chi Lee[1,4]
[1]Department of Molecular and Human Genetics
Baylor College of Medicine
One Baylor Plaza
Houston, Texas 77030
[2]Department of Molecular Pathology
[3]Department of Pathology
Division of Pathology and Laboratory Medicine
M. D. Anderson Cancer Center
The University of Texas
1515 Holcombe Boulevard
Houston, Texas 77030

Summary

The *Period2* gene plays a key role in controlling circadian rhythm in mice. We report here that mice deficient in the *mPer2* gene are cancer prone. After γ radiation, these mice show a marked increase in tumor development and reduced apoptosis in thymocytes. The core circadian genes are induced by γ radiation in wild-type mice but not in *mPer2* mutant mice. Temporal expression of genes involved in cell cycle regulation and tumor suppression, such as *Cyclin D1, Cyclin A, Mdm-2*, and *Gadd45α,* is deregulated in *mPer2* mutant mice. In particular, the transcription of c-*myc* is controlled directly by circadian regulators and is deregulated in the *mPer2* mutant. Our studies suggest that the *mPer2* gene functions in tumor suppression by regulating DNA damage-responsive pathways.

Introduction

Circadian rhythms are the daily oscillations of multiple biological processes driven by endogenous clocks. The master circadian clock in mammals resides in the suprachiasmatic nucleus (SCN) of the anterior hypothalamus. To date, eight core circadian genes have been identified. They are *Casein kinase 1ε* (*CK1ε*); *Cryptochrome1* (*Cry1*) and *Chryptochrome2* (*Cry2*); *Period1 (Per1), Period2* (*Per2)*, and *Period3 (Per3)*; *Clock*; and *Bmal1*. The three *Per* genes encode PER-ARNT-SIM (PAS) domain proteins that function in the nucleus but do not directly bind to DNA. The *Clock* and *Bmal1* genes encode basic-helix-loop-helix (bHLH)-PAS transcription factors. The levels of mRNAs and proteins of these genes, except those of *Clock* and *CK1ε,* oscillate robustly during 24 hr circadian periods (Reppert and Weaver, 2001; Young and Kay, 2001).

The molecular clockwork in the SCN is composed of interacting positive and negative feedback loops of clock genes. In the best-known positive feedback loop, the transcription of *Per2* is directly activated by BMAL1/CLOCK heterodimers, whereas the nuclear PER2 stimulates *Bmal1* transcription through PAS-mediated reactions with other transcription factors. In the best-known negative feedback loop, cytoplasmic CRY1 regulates PER2 stability and nuclear translocation, while nuclear CRY1 suppresses *Per2* transcription by inhibiting the activity of BMAL1/CLOCK heterodimers directly (Reppert and Weaver, 2001; Young and Kay, 2001).

Molecular clockwork similar to that in SCN neurons has been found in all peripheral tissues studied (Zylka et al., 1998) and can be induced in cultured fibroblasts (Balsalobre et al., 1998). It has been shown recently that the neuronal PAS domain protein 2 (NPAS2), a bHLH-PAS transcription factor that is highly related to CLOCK in amino acid sequence, is also a bona fide partner of BMAL1 (Reick et al., 2001; Rutter et al., 2001). The NPAS2/BMAL1 heterodimers, as part of the molecular clock, control the expression of targeted genes in mouse forebrain and vascular cells (Reick et al., 2001; McNamara et al., 2001). The circadian clock controls downstream events by regulating the expression of clock-controlled genes (CCGs) that function in the rate-limiting steps of various biological pathways (Panda et al., 2002).

Several lines of in vivo observation indicate that the circadian clock may play a role in growth control as well. First, cell proliferation and apoptosis in rapidly renewing tissues are circadian synchronized (Bjarnason and Jordan, 2000; Ruifrok et al., 1998). Second, the proliferation of tumor cells follows autonomous circadian patterns that are out of phase with nontumor cells (Klevecz et al., 1987; Barbason et al., 1995). Third, irregular circadian cycles, such as night-shift work in humans or constant exposure to light in rodents, increase mammary tumorigenesis (Hansen, 2001; Anderson et al., 2000). Circadian genes may also respond directly to genotoxic stress, since sleep disorder is common among patients receiving radiation treatment and chemotherapy (Winningham, 2001), and the timing of chemotherapy is associated with efficacy and toxicity of the treatment (Hrushesky, 2001).

We have shown previously that mice homozygous for the *mPer2* mutation (*mPer2$^{m/m}$*) are deficient in circadian clock function (Zheng et al., 1999). The mutant *mPer2* carries an in-frame deletion in the PAS-B domain and is deficient in *mPer2*-mediated transcription regulation (Zheng et al., 2001). These mice provide an ideal model to test the role of circadian genes in growth control and DNA damage response in vivo.

We report here that *mPer2$^{m/m}$* mice show a neoplastic growth phenotype and an increased sensitivity to γ radiation, manifested by premature hair graying, increased tumor occurrence, and reduced apoptotic response in thymocytes. The core circadian genes are induced by γ radiation in wild-type but not in *mPer2$^{m/m}$* mice. The expression of genes functioning in cell proliferation and tumor suppression, such as *Cyclin D1, Cyclin A*, *Mdm-2,* and *Gadd45α*, follows distinct circadian patterns in vivo and is deregulated in *mPer2$^{m/m}$* mice. In particular, the circadian regulators control c-*myc* gene transcription directly through E box-mediated reactions. We propose that the circadian clock suppresses cancer develop-

[4]Correspondence: ching@bcm.tmc.edu

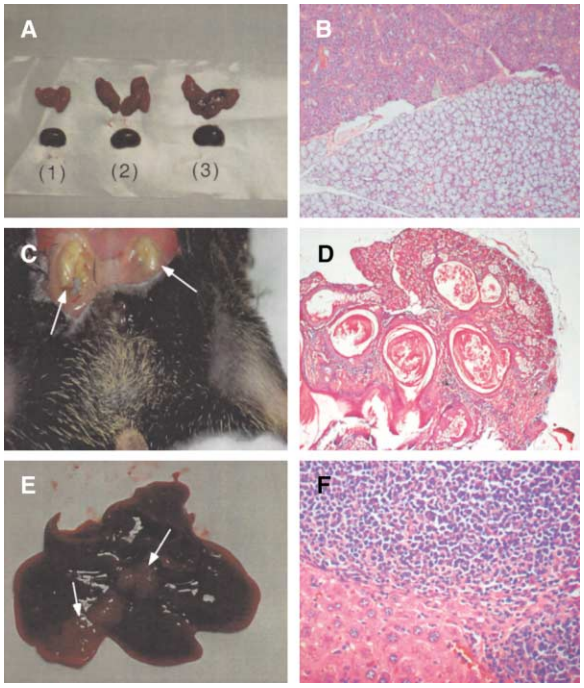

Figure 1. Hyperplastic Growth and Radiation-Induced Lymphoma in *mPer2*$^{m/m}$ Mice

(A) Salivary gland hyperplasia in unirradiated *mPer2*$^{m/m}$ mice: salivary gland and kidney (for size comparison) from (1) an 8-month-old wild-type mouse, (2) an 8-month-old *mPer2*$^{m/m}$ mouse, and (3) an 18-month-old *mPer2*$^{m/m}$ mouse. Note: salivary gland hyperplasia is more evident in the older *mPer2*$^{m/m}$ mouse.

(B) Hyperplasia of major and minor salivary glands from an unirradiated *mPer2*$^{m/m}$ mouse (4 × 10).

(C) Gross photo of teratoma in an unirradiated male *mPer2*$^{m/m}$ mouse.

(D) Mature cystic teratoma of hyperkeratotic skin with subaceous glands shown in (C) (10 × 10).

(E) Malignant lymphoma in the liver of an irradiated *mPer2*$^{m/m}$ mouse.

(F) Histology of the lymphoma (40 × 10) shown in (E).

ment in vivo by regulating the expression of CCGs that function in growth control and DNA damage response.

Results

mPer2 Mutant Mice Show Increased Sensitivity to γ Radiation and Tumor Development

Newborn *mPer2*$^{m/m}$ mice are morphologically normal. Histological examination at the age of 6 months did not reveal abnormalities in most organ systems, except that the *mPer2*$^{m/m}$ mice began to show salivary gland hyperplasia in both males and females (Figures 1A and 1B) and teratomas, predominantly of the epidermis (Figures 1C and 1D) in males. By the age of 12 months, all *mPer2*$^{m/m}$ mice showed salivary gland hyperplasia and all male *mPer2*$^{m/m}$ mice developed teratomas around the genital areas (Table 1). In addition, 30% of *mPer2*$^{m/m}$ mice studied died before the age of 16 months, with the first case at 9 months of age. Pathological analysis showed that 15% of the *mPer2*$^{m/m}$ mice died of lymphoma. Hyperplasia was not observed in wild-type control mice at 18 months of age, and spontaneous lymphoma in wild-type mice was first found at the age of 20 months (Table 1). The frequency of neoplasia in *mPer2*$^{m/m}$ mice differs significantly from wild-type mice ($p < 0.0001$, t test). Thus, the *mPer2*$^{m/m}$ mice are cancer prone.

To examine further the role of *mPer2* in suppressing neoplastic growth, wild-type and *mPer2*$^{m/m}$ mice at 8 weeks of age were challenged with a single dose of whole-body γ radiation of 4 Gy at zeitgeber time 10 (ZT10) and were monitored for illness and survival. Mice were irradiated at ZT10 because the mitotic index is highest in murine bone marrow between ZT8 and ZT12 (Bjarnason and Jordan, 2000) and cells in mitosis are more sensitive to γ radiation (Wood et al., 1998).

The *mPer2*$^{m/m}$ mice are more sensitive to γ radiation, as indicated by premature hair graying and hair loss, and an increased rate of tumor formation. Hair graying was observed in 50% of mutant mice at 12 weeks after irradiation. At 22 weeks after irradiation, all the irradiated *mPer2*$^{m/m}$ mice showed hair graying, and 30% of them also showed large areas of hair loss on the back (Figure 2A) or around neck and mouth. In contrast, hair graying and hair loss was not found in any wild-type mice at 22 weeks after irradiation (Figure 2B). The irradiated *mPer2*$^{m/m}$ mice also showed an earlier onset of hyperplastic growth. At 7 months after irradiation, teratoma was observed in all irradiated male *mPer2*$^{m/m}$ mice, but not in any irradiated wild-type mice.

The *mPer2*$^{m/m}$ mice show a significantly higher frequency of tumor development than wild-type mice after irradiation ($p < 0.0001$, t test). At 16 months after irradiation, 71% of irradiated *mPer2*$^{m/m}$ mice developed malignant lymphoma, with the first case found at 5 months after irradiation (Figure 2C, Table 1). Complete necropsies were performed on mice that showed severe morbidity. The time of death was estimated within 1 week of autopsy. Histological examination demonstrated that all irradiated *mPer2*$^{m/m}$ mice that showed severe morbidity had malignant lymphomas in multiple organs including liver, lung, spleen, heart, ovary, salivary gland, muscle, pancreas, stomach, intestines, testis, and bone (Figures 1E and 1F). In contrast, at 16 months after irradiation, only 5% of irradiated wild-type mice developed malignant lymphoma. Another 10% of irradiated wild-type mice developed angiosarcoma. One of them was euthanized at 9 months and another at 15 months after irradiation (Figure 2C, Table 1).

mPer2$^{m/m}$ Thymocytes Show Reduced Apoptosis in Response to γ Radiation

Apoptosis is essential for suppressing malignant growth after genomic DNA damage. The high frequency of malignant lymphoma in irradiated *mPer2*$^{m/m}$ mice suggested that *mPer2*$^{m/m}$ lymphoid cells might be deficient in radiation-induced apoptosis. To test this hypothesis, wild-type and *mPer2*$^{m/m}$ mice at 4 weeks of age were treated with 4 Gy of γ radiation at ZT10. Thymus was isolated from the mice at various times after irradiation. Half of the thymus was fixed for histological examination, and thymocytes from the other half of the thymus were examined by flow cytometry.

Histological examination revealed that thymocytes were depleted from wild-type thymus in a time-dependent manner after irradiation, resulting in the loss of

Table 1. Neoplastic Growth Phenotypes of *mPer2*$^{m/m}$ Mice

Phenotypes	*mPer2*$^{m/m}$ Mice (18 months old) (n = 20)	Wild-Type Mice (18 months old) (n = 20)	*mPer2*$^{m/m}$ Mice 16 months after IR (n = 14[a])	Wild-Type Mice 16 months after IR (n = 20)	p value
Salivary gland hyperplasia	20 (50%)[b]	0	14 (100%)	1 (5%)	<0.0001
Teratoma in male mice	10 (100%)	0	9 (100%)	0	
Hair graying 6 months after IR			14 (100%)	0	
Lymphoma	3 (15%)	0	10 (71%)	1 (5%)	<0.0001
Angiosarcoma	0	0	0	2 (10%)	

[a] Six irradiated *mPer2*$^{m/m}$ mice were lost at 9 months after irradiation during the summer flooding in Houston in 2001.
[b] 50% of *mPer2*$^{m/m}$ mice showed enlarged salivary glands by physical examination. At autopsy, all the *mPer2*$^{m/m}$ mice older than 8 month of age were found to have salivary gland hyperplasia.

lymphoid tissue at 18 hr after irradiation. In contrast, *mPer2*$^{m/m}$ thymus still retained a substantial number of thymocytes at 18 hr after irradiation (Figure 3A). Flow cytometry indicated that the ratio of apoptotic thymocytes was about 2-fold higher in wild-type thymus than in *mPer2*$^{m/m}$ thymus at 10 and 18 hr after irradiation (Figure 3A). Apoptotic cells were still detected by flow cytometry in wild-type but not in *mPer2*$^{m/m}$ thymus at 22 hr after irradiation, and were not detected in either wild-type or *mPer2*$^{m/m}$ thymus at 24 hr after irradiation in repeated experiments (data not shown). Thus, the *mPer2*$^{m/m}$ thymocytes were more resistant to apoptosis when irradiated at ZT10.

To investigate whether *mPer2* mutation resulted in resistance to radiation-induced apoptosis at other ZT times, mice were irradiated at ZT2 or ZT18. Thymus was isolated from the irradiated mice at 18 hr after irradiation. Histological examination revealed that when irradiated at ZT2, almost all wild-type thymocytes were eliminated by apoptosis within 18 hr, and only connective tissues and spindle cell types remained in the thymus. When irradiated at ZT18, most wild-type thymocytes were depleted in 18 hr, and only a few intact thymocytes were identified on the histological slides. In contrast, a large number of intact *mPer2*$^{m/m}$ thymocytes were present in the thymus at 18 hr after irradiation in the same experiments (Figure 3B). Flow cytometry showed that when irradiated at ZT2 or ZT18, no intact wild-type thymocytes could be isolated at 18 hr after irradiation following standard procedures, whereas many *mPer2*$^{m/m}$ thymocytes were recovered and examined (Figure 3B). A striking discovery from flow cytometry analysis was that *mPer2*$^{m/m}$ thymocytes also responded to γ radiation differently at different ZT times: when irradiated at ZT10, they were more resistant to apoptosis at every phase of cell cycle, whereas when irradiated at ZT2 or ZT18, they arrested at G2/M to survive (Figures 3A and 3B). Thus, mouse thymocytes are most sensitive to γ radiation in early sleeping phase (ZT2), less sensitive in active phase (ZT18), and the least sensitive in late sleeping phase (ZT10). Mutation in *mPer2* results in a partial resistance to radiation-induced apoptosis at all ZT times.

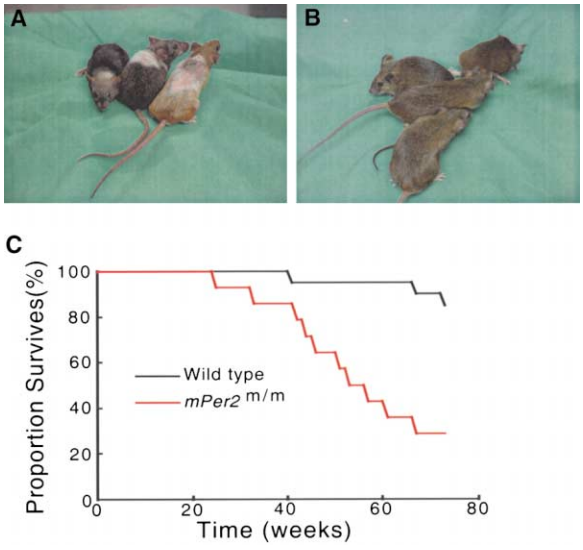

Figure 2. *mPer2*$^{m/m}$ Mice Show Increased Sensitivity to γ Radiation
(A) All the irradiated *mPer2*$^{m/m}$ mice show hair graying at 22 weeks after irradiation. Some of them also show hair loss on the back.
(B) Wild-type mice at 22 weeks after irradiation.
(C) Survival curve for wild-type and *mPer2*$^{m/m}$ mice after irradiation.

Wild-type thymocytes undergo rapid apoptosis after γ radiation in a p53-dependent manner (Lowe et al., 1993; Clarke et al., 1993). To test whether the deficiency in p53 induction plays a role in the apoptotic resistance of *mPer2*$^{m/m}$ thymocytes after irradiation, the accumulation of p53 protein in these cells was examined. Thymocytes were isolated from wild-type and *mPer2*$^{m/m}$ mice at 4 weeks of age and treated with 4 Gy of γ radiation. Protein extracts of these cells were prepared at various times after irradiation. The level of p53 in cell extracts was determined by Western blot analysis. As shown in Figure 4A, the induction of p53 was evident in wild-type thymocytes at 4 hr after irradiation and further increased at 6 hr after irradiation. In *mPer2*$^{m/m}$ thymocytes, however, the induction of p53 followed much slower kinetics, and only reached 60% and 40% of that in the wild-type thymocytes at 4 and 6 hr after irradiation, respectively. Thus, p53 induction is attenuated in *mPer2*$^{m/m}$ thymocytes after irradiation.

In p53-dependent apoptosis, cytochrome c is released from mitochondria into cytosol, where it interacts with Apaf-1 to activate downstream caspases (Green and Reed, 1998). To examine whether the deficiency in p53 induction after γ radiation could lead to decreased cytochrome c release in *mPer2*$^{m/m}$ thymocytes, the level of cytochrome c in mitochondria of wild-type and *mPer2*$^{m/m}$ thymocytes was analyzed by Western blot analysis. As shown in Figure 4B, cytochrome c levels in the mitochondria of wild-type thymocytes decreased

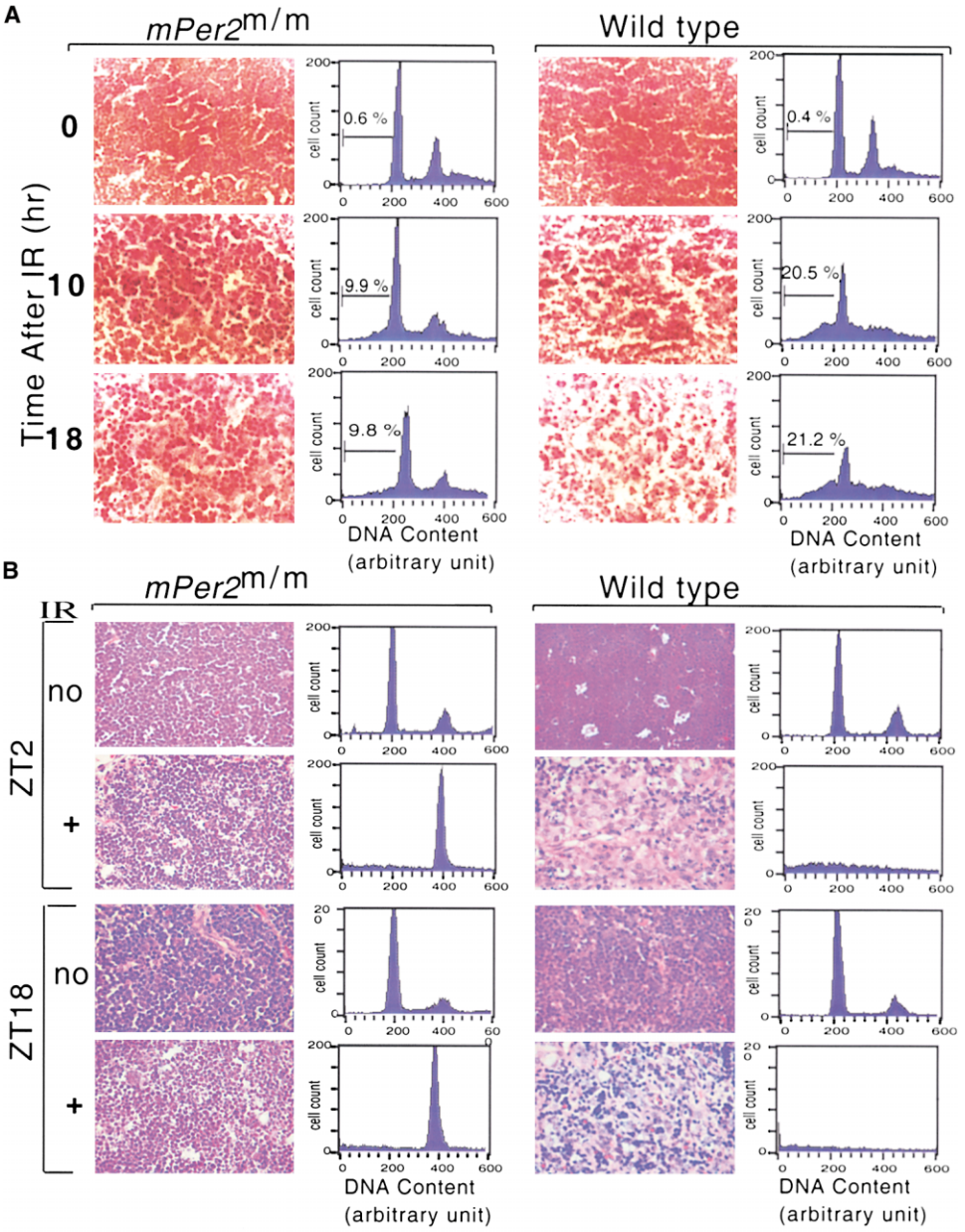

Figure 3. The *mPer2*$^{m/m}$ Lymphocytes Show Reduced Apoptosis after γ Radiation

(A) Wild-type and *mPer2*$^{m/m}$ mice were irradiated with 4 Gy at ZT10. Thymus was isolated from unirradiated and irradiated mice at 10 and 18 hr after irradiation. Half of the thymus was fixed for histological analysis (40 × 10). Thymocytes from the other half of the thymus were analyzed by flow cytometry. Percentages of apoptotic cells detected by flow cytometry are shown in histograms. The results of flow cytometry from three independent experiments are consistent in showing that radiation-induced apoptosis in *mPer2*$^{m/m}$ thymocytes is about 2-fold less efficient than in wild-type thymocytes. The results of histological analysis and flow cytometry from one of the three experiments are presented side-by-side.

(B) The experiments described in (A) were repeated at ZT2 and ZT18, and the apoptosis of wild-type and *mPer2*$^{m/m}$ thymocytes were examined at 18 hr after irradiation. The results from repeated experiments are similar. The results from one of the experiments are presented side-by-side.

dramatically after irradiation: about 50% of cytochrome c was released into the cytosol at 6 hr after irradiation, and only 10% of cytochrome c still remained in mitochondria at 16 hr after irradiation. In contrast, mitochondria in *mPer2*$^{m/m}$ thymocytes retained more than 85% of their cytochrome c at 6 hr after irradiation and about 38% of their cytochrome c at 16 hr after irradiation (Figure 4B). Thus, the partial resistance to γ radiation-induced apoptosis in *mPer2*$^{m/m}$ thymocytes likely results from deficiencies in p53-mediated cytochrome c release.

Mammalian Circadian Genes Are Induced by γ Radiation

Increased radiosensitivity in *mPer2*$^{m/m}$ mice indicates that mammalian clock genes may respond directly to γ radiation to maintain homeostasis. Mutations in *mPer2*

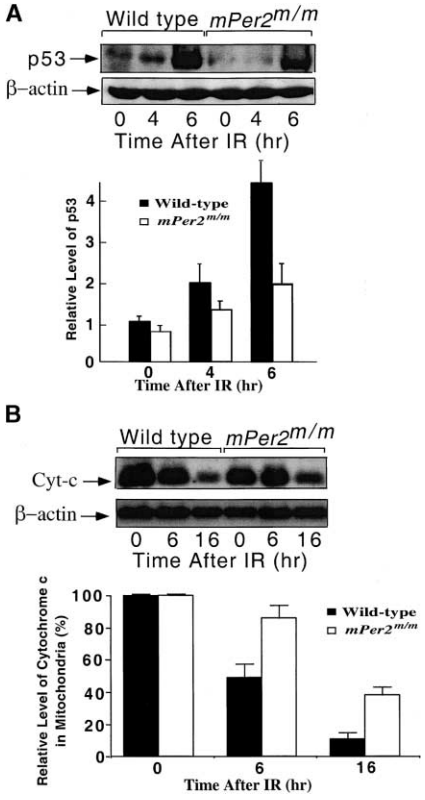

Figure 4. The *mPer2*$^{m/m}$ Thymocytes Are Deficient in p53 Protein Induction and Cytochrome c Release after γ Radiation

(A) p53 induction after γ radiation is attenuated in *mPer2*$^{m/m}$ thymocytes. Thymocytes were isolated from wild-type and *mPer2*$^{m/m}$ mice and were treated with 4 Gy of γ radiation. Cell extracts were prepared from unirradiated cells and irradiated cells at 4 and 6 hr after irradiation. The level of p53 protein was detected by Western blot analysis using a p53-specific antibody PAb421 and was normalized to the level of β-actin using a Molecular Dynamics densitometer. The ratio of p53 signal to β-actin signal in the lysates prepared from unirradiated wild-type thymocytes was arbitrarily set as 1.0. Error bars indicate standard error of the mean (SEM) (n = 6).

(B) Cytochrome c release after γ radiation is inefficient in *mPer2*$^{m/m}$ thymocytes. Thymocytes were isolated from wild-type and *mPer2*$^{m/m}$ mice and were treated with 4 Gy of γ radiation. The mitochondrial fraction was prepared from unirradiated cells and irradiated cells at 6 and 16 hr after irradiation. The level of cytochrome c was determined by Western blot analysis and was normalized to the level of β-actin. The ratio of cytochrome c signal to β-actin signal in the lysates prepared from unirradiated thymocytes was arbitrarily set as 1.0. Error bars indicate SEM (n = 4).

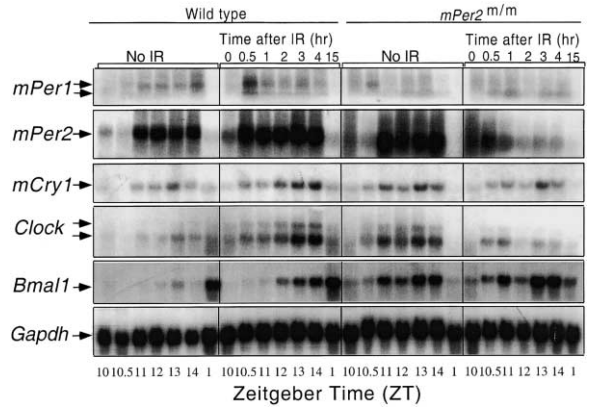

Figure 5. Mammalian Clock Genes Are Early Responsive Genes to γ Radiation

Wild-type and *mPer2*$^{m/m}$ mice were treated with 4 Gy of γ radiation at ZT10. Total RNA was isolated from the livers of irradiated and unirradiated mice at ZT10, ZT10.5, ZT11, ZT12, ZT13, ZT14, and ZT1 of the subsequent day. The RNA samples were analyzed by Northern hybridization. The blots were hybridized sequentially with ^{32}P-labeled *mPer1, mPer2, Bmal1, Clock, Cry1*, and *Gapdh* cDNAs.

may abolish such a response. To test this hypothesis, wild-type and *mPer2*$^{m/m}$ mice at 10 to 12 weeks of age were treated with 4 Gy of γ radiation at ZT10. Total RNA was extracted from the livers of unirradiated and irradiated mice at ZT10, ZT10.5, ZT11, ZT12, ZT13, ZT14, and at ZT1 of the subsequent day. The abundance of transcripts from five core clock genes, *Clock, Bmal1, mPer1, mPer2*, and *Cry1*, was determined by Northern blot analysis. The results are shown in Figure 5 and Supplemental Figure S1 at http://www.cell.com/cgi/content/full/111/1/41/DC1.

In the livers of unirradiated wild-type mice, the transcripts of the core circadian genes are expressed in gene-specific patterns from ZT10 to ZT1. γ radiation induced a rapid and gene-specific increase in the levels of all these transcripts: the *mPer1, mPer2, Clock*, and *Cry1* genes were induced within 30 min of irradiation, and the *Bmal1* gene was induced in 2 hr. The induction of *Bmal1, Clock*, and *Cry1* followed slower kinetics but persisted longer (more than 4 hr) when compared with that of *mPer1* and *mPer2* (less than 2 hr). The induction of circadian genes by γ radiation at ZT10 was transient: by 15 hr after irradiation at ZT1, the levels of all circadian transcripts studied, except that of *Bmal1* mRNA, returned to the basal level. In contrast, in the livers of irradiated *mPer2*$^{m/m}$ mice, γ radiation did not significantly alter the expression of most circadian genes, but did suppress the expression of the 6.6 kb *mPer1*, the *mPer2*, and the two *Clock* mRNAs (Figure 5 and Supplemental Figure S1).

It is unclear at present whether the induction of circadian genes after γ radiation in wild-type mouse livers is still controlled by the feedback loops of clock genes. However, mutation in *mPer2* abolished the induction of all clock genes studied, indicating that the core circadian genes respond to γ radiation in a coordinated manner in vivo.

Circadian Clock-Controlled Genes Are Involved in Cell Cycle Control and Tumor Suppression

The circadian clock controls downstream events by regulating the expression of CCGs. We postulate that certain genes that function in cell proliferation and tumor suppression are CCGs and are deregulated in *mPer2*$^{m/m}$ mice. To test this hypothesis, total RNA was extracted from the livers of wild-type and *mPer2*$^{m/m}$ mice at ZT2, ZT6, ZT10, ZT14, ZT18, and ZT22. The levels of mRNAs of several candidate genes were examined by Northern blot analysis. The results of three independent experiments are summarized and presented in Figure 6 and Supplemental Figure S2 at http://www.cell.com/cgi/content/full/111/1/41/DC1.

The first gene examined was the protooncogene c-*myc*. The c-*myc* gene was selected because (1) c-Myc

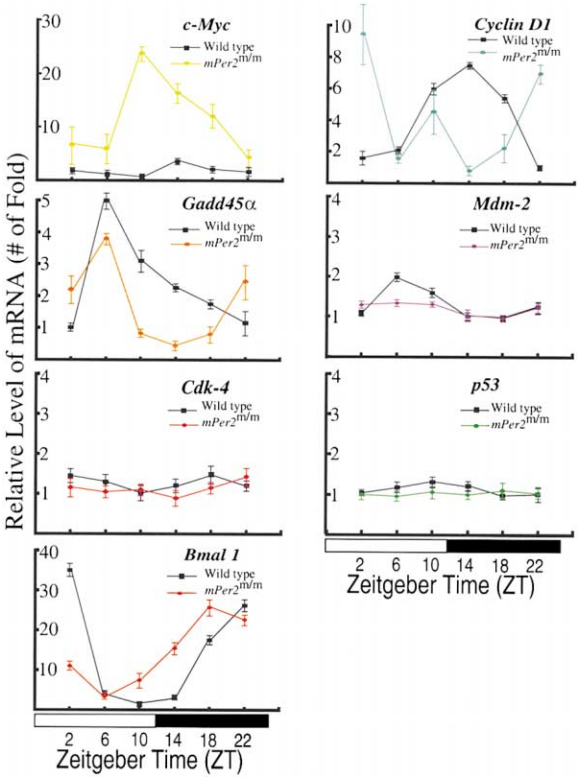

Figure 6. Expression of c-*myc, p53, Cdk4, Cyclin D1, Mdm-2, Gadd45*α, *Bmal1*, and *Gapdh* mRNAs in Mouse Livers

Summary of three Northern blots analysis on the expression of c-*myc, p53, Cdk4, Cyclin D1, Mdm2*, *Gadd45*α, *Bmal1*, and *Gapdh* mRNAs in mouse liver. Each mRNA band was quantified using a Molecular Dynamics densitometer. All values were normalized to *Gapdh* RNA to ensure an equivalent loading of RNA on the blots. The ratio of each mRNA signal to *Gapdh* mRNA signal at the trough of its oscillation was arbitrarily set as 1.0. Error bars indicate SEM (n = 3).

plays a key role in cell proliferation and apoptosis (Evan and Vousden, 2001); (2) c-Myc is a transcription factor and possesses a bHLH motif that interacts with the E box sequences in the promoter of a target gene (Blackwell et al., 1993); and (3) the bHLH motif is also found in NPAS2, CLOCK, and BMAL1. Therefore, circadian regulators may target genes that are controlled by c-*myc*. c-*myc* itself may be controlled by the circadian clock as well, since it contains multiple consensus E box sequences in the P1 promoter (Battey et al., 1983). Northern blot analysis showed that the level of c-*myc* mRNA oscillated in 24 hr L/D cycles in wild-type mouse livers, with the trough at ZT10 and the peak at ZT14. In *mPer2*$^{m/m}$ livers, however, the c-*myc* mRNA showed an oscillating pattern from ZT10 to ZT22, but not from ZT2 and ZT6, and was consistently elevated at all ZT times studied (Figure 6). Thus, c-*myc* is a CCG and its expression is deregulated in *mPer2*$^{m/m}$ mice.

We next examined the expression of the *myc*-controlled genes *Cyclin D1* and *Gadd45*α. The level of *Cyclin D1* mRNA was at its trough at ZT22 and peaked at ZT14 in wild-type mouse livers, but showed no oscillating pattern in *mPer2*$^{m/m}$ mouse livers (Figure 6). The trough of *Gadd45*α mRNA in wild-type livers was at ZT2 and the peak at ZT6. In *mPer2*$^{m/m}$ livers, *Gadd45*α mRNA expression still peaked at ZT6 but reached only 80% of the level in wild-type livers. Subsequently, the level of *Gadd45*α mRNA at ZT10, ZT14, and ZT18 was significantly lower and only reached 20%, 17%, and 44% of that in wild-type livers, respectively (Figure 6). These results indicate that *Cyclin D1* and *Gadd45*α are under circadian control in vivo.

Not all *myc*-target genes are controlled by the circadian clock at the mRNA level. For example, the expression of *Cdk-4* and *p53* mRNAs did not oscillate during 24 hr L/D cycles in wild-type livers. As a consequence, mutations in *mPer2* had no effect on the expression of these mRNAs (Figure 6). At posttranscriptional levels, however, *p53* might still be controlled by circadian clock in vivo (Bjarnason et al., 1999). One of the genes involved in posttranscriptional regulation of *p53* is *Mdm-2*. The level of *Mdm-2* mRNA showed a moderate oscillation in 24 hr L/D cycles in wild-type mouse livers, with the peak at ZT6 and the trough at ZT14, but was dampened in *mPer2*$^{m/m}$ mouse livers (Figure 6).

The level of *Bmal1* mRNA in each RNA sample was determined so that it could serve as an internal control for circadian regulation. In wild-type mouse livers, the level of *Bmal1* mRNA peaked at ZT2 and reached the trough at ZT10. In *mPer2*$^{m/m}$ mouse livers, the trough of *Bmal1* mRNA was at ZT6 and the peak at ZT18, but the peak level of *Bmal1* mRNA was only 70% of that in wild-type livers at ZT2 (Figure 6). Thus, as has been found in mouse SCN (Shearman et al., 2000), the expression of *Bmal1* mRNA in *mPer2*$^{m/m}$ livers still oscillates in 24 hr L/D cycles, but with a phase shift and a decrease in amplitude compared to the pattern in wild-type mouse livers.

The NPAS2/BMAL1 Heterodimers Suppress c-*myc* Promoters Directly

To examine whether circadian regulators control c-*myc* transcription directly, we performed transient transfection assays. Three reporter constructs were used in this study. The *mPer1*-Luc is a luciferase reporter driven by the 7.2 kb *mPer1* promoter (Yamaguchi et al., 2000). The XNM-Luc is a luciferase reporter driven by the human c-*myc* P2 minimal promoter that does not contain the E box sequence (Facchini et al., 1997). The SNM-Luc is a luciferase reporter driven by both the c-*myc* P1 and P2 promoters (Facchini et al., 1997) that contain two E box consensus sequences (Blackwell et al., 1993; Battey et al., 1983).

The *mPer2*$^{m/m}$ embryonic fibroblasts (MEFs) were transfected with the three reporters in separate experiments. As has been shown previously (Reick et al., 2001), coexpression of the *mPer1*-Luc reporter with either BMAL1 or NPAS2 alone had little effect on promoter activity, whereas coexpression of both BMAL1 and NPAS2 with the *mPer1*-Luc reporter resulted in a dose-dependent increase in reporter activity. Activation of the *mPer1*-Luc reporter by BMAL1/NPAS2 heterodimers was repressed by CRY1 in a dose-dependent manner (Figure 7A). Thus, the BMAL1/NPAS2 heterodimers activate the *mPer1* promoter, whereas CRY1 represses it by inhibiting the activity of BMAL1/NPAS2 heterodimers. The XNM-Luc reporter plasmid did not respond to any

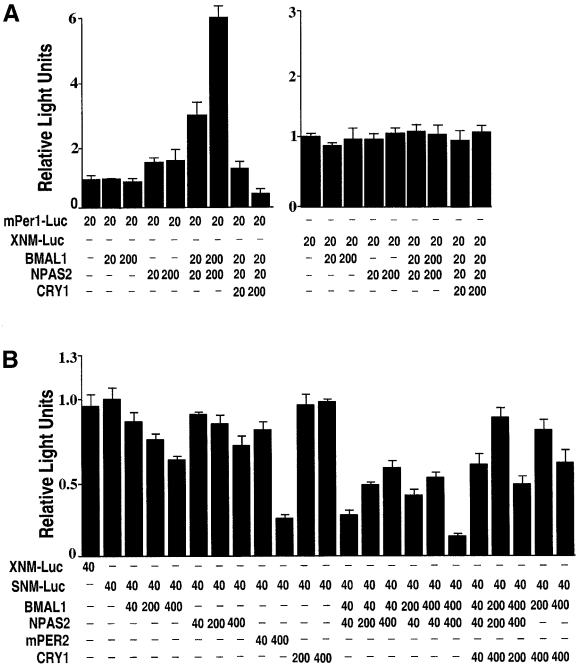

Figure 7. Transient Transfection Assays Monitoring the Effects of Circadian Regulators on the c-*myc* Promoters

(A) *mPer2*$^{m/m}$ MEFs were transfected with an invariant 20 ng dose of *mPer1*-Luc or XNM-Luc plasmid, along with varying amount of *Npas2, Bmal1,* and *Cry1* expression vectors as indicated. Cells were harvested at 24 hr after transfection and assayed for luciferase activity. The level of luciferase activity in samples transfected with reporter plasmid alone was arbitrarily set as 1.0. Error bars indicate SEM (n = 3).

(B) *mPer2*$^{m/m}$ MEFs were transfected with an invariant 40 ng dose of SNM-Luc or XNM-Luc plasmid, along with varying amount of *Npas2, Bmal1, Cry1*, and *mPer2* expression vectors as indicated. Cells were harvested at 24 hr after transfection and assayed for luciferase activity. The level of luciferase activity in samples transfected with the SNM-Luc plasmid alone was arbitrarily set as 1.0. Error bars indicate SEM (n = 6).

of the circadian regulators in similar transfection assays (Figure 7A).

Compared to the *mPer1*-Luc reporter, the circadian regulators had a precisely opposite effect on the SNM-Luc reporter. Coexpression of the SNM-Luc reporter with either BMAL1 or NPAS2 alone resulted in a mild decrease in promoter activity. The dose-dependent inhibition of the SNM-Luc reporter became evident, when BMAL1 and NPAS2 were coexpressed in cells, and could be relieved by CRY1 in a dose-dependent manner. CRY1, by itself, had no effect on SNM-Luc reporter activity nor did it relieve the mild inhibition of the SNM-Luc reporter by BMAL1 alone (Figure 7B). Therefore, the BMAL1/NPAS2 heterodimers suppress c-*myc* transcription, presumably through E box-mediated reactions in the c-*myc* gene P1 promoter, whereas CRY1 can relieve such suppression by inhibiting the activity of BMAL1/NPAS2 heterodimers.

Discussion

We have shown previously that *mPer2*$^{m/m}$ mice display a shorter circadian period that is followed by the loss of persistence in circadian rhythmicity in constant darkness (Zheng et al., 1999). A similar abnormal circadian phenotype is observed in *mPer2* null mice that were generated independently (Bae et al., 2001). Recently, we have also generated *mPer2*$^{-/-}$ mice (see Supplemental Figures S3A and S3B at http://www.cell.com/cgi/content/full/111/1/41/DC1) that display a similar circadian phenotype (data not shown) and a similar neoplastic growth phenotype to the *mPer2*$^{m/m}$ mice. Salivary gland hyperplasia was observed in some of *mPer2*$^{-/-}$ mice at 4 months of age. At 7 months of age, most of the *mPer2*$^{-/-}$ mice examined had enlarged salivary glands (Supplemental Figure S3C). In addition, *mPer2*$^{-/-}$ thymocytes show a partial resistance to apoptosis after γ radiation as *mPer2*$^{m/m}$ thymocytes (Supplemental Figure S3D). Taken together, these studies demonstrate that the in-frame deletion mutant *mPer2*$^{m/m}$ mice have the same phenotype as the null mutant *mPer2*$^{-/-}$ mice in controlling circadian behavior as well as in growth regulation and DNA damage response.

Recent studies have revealed that, in vivo, a large number of genes are controlled by the circadian clock in a tissue-specific manner and that many of these CCGs function in the rate-limiting steps of major physiological processes (Panda et al., 2002; Kornmann et al., 2001; Zheng et al., 2001). It is likely that deregulation of multiple molecular pathways contribute to the cancer prone phenotype and the deficiencies in DNA damage response in *mPer2* mice. In our study, we have focused on studying the circadian clock-controlled c-*myc* and *p53* expression to highlight the fundamental role that the circadian clock plays in tumor suppression.

p53 levels increase in response to genotoxic stress through posttranscriptional mechanisms (Giaccia and Kastan, 1998). Studies of p53 posttranslational stabilization reveal that DNA-dependent protein kinases, ATM and CHK2, are activated by γ radiation and phosphorylate p53 at N-terminal sites near the region for MDM2 binding, leading to p53 stabilization (Vogelstein et al., 2000). In mouse livers, mutations in *mPer2* have no apparent effect on p53 mRNA expression, but dampen the circadian oscillation of *Mdm2* mRNA and result in a high level of MDM2 throughout 24 hr L/D cycles (Figure 6 and see Supplemental Figure S4 at http://www.cell.com/cgi/content/full/111/1/41/DC1). The mechanism responsible for the reduced p53 induction in *mPer2*$^{m/m}$ thymocytes after γ radiation is still not fully understood. However, the striking difference in radiation-induced apoptosis at different ZT times in both wild-type and *mPer2*$^{m/m}$ thymocytes shown in Figure 3 indicates that apoptotic response to γ radiation in vivo is strictly controlled by the circadian clock. A large number of CCGs in various regulatory pathways may be involved, and among them the *p53* gene plays an important role in this regulation.

Deregulation of c-*myc* has been linked to various cancers, as well as to hyperplastic growth of mammalian tissues (Sherr, 1996; Hecht and Aster, 2000). Mutations in *mPer2* lead to deregulation of c-*myc* in all mouse tissues studied and results in salivary gland hyperplasia. Studies of cell cycle gene expression in mouse livers and salivary glands indicate that mouse salivary glands express additional cell cycle genes that are not detected in livers, such as *Cyclin A*, which is also deregulated

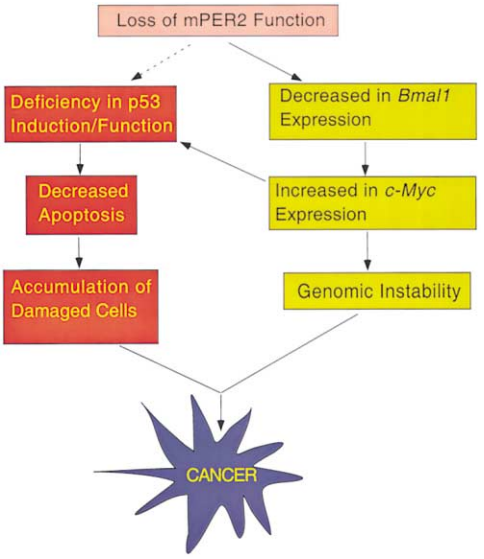

Figure 8. A Proposed Model for the Role of *mPer2* in Tumor Suppression

The solid lines indicate the pathways that have been demonstrated by our study as well as by the studies of others. The dashed line indicates a regulatory pathway(s) that is still not fully understood at present.

upon *mPer2* mutation (see Supplemental Figure S5 at http://www.cell.com/cgi/content/full/111/1/41/DC1). Thus, the loss of circadian control of c-*myc* expression has profound effect on certain types of tissues, such as salivary gland, in vivo.

The transcription of c-*myc* in mammalian cells is initiated from the two major start sites, P1 and P2. The majority of c-*myc* transcripts arise from the P2 promoter (Spencer and Groudine, 1991). It has been proposed that the low level of c-*myc* transcription in normal cells was a result of repression of the P2 promoter (Lee and Ziff, 1999; Facchini et al., 1997). In our studies, the c-*myc* P2 minimal promoter did not respond to circadian regulators, whereas the promoter activity of the c-*myc* 5′ sequence containing both P1 and P2 was suppressed by BMAL1/NPAS2 heterodimers (Figure 7B). Thus, the BMAL1/NPAS2 or BMAL1/CLOCK heterodimers likely repress transcription of c-*myc* through E box-mediated reactions in the P1 promoter, and *mPer2* can suppress c-*myc* expression indirectly through stimulating *Bmal1* transcription. Deregulation of *Bmal1* in *mPer2*$^{m/m}$ cells, therefore, results in c-*myc* overexpression (Figure 6 and see Supplemental Figure S2 at http://www.cell.com/cgi/content/full/111/1/41/DC1).

The c-Myc protein plays an important role in both cell proliferation and apoptosis. Oncogenic transformation mediated by c-*myc* must therefore overcome its proapoptotic activity (You et al., 2002), in which modulation of p53-mediated apoptosis plays an important role (Pucci et al., 2000; Evan and Vousden, 2001). It has been shown that suppression of *myc*-induced apoptosis in *myc*-overexpressing cells is sufficient to initiate tumor development without additional neoplastic lesions (Pelengaris et al., 2002). In addition, c-*myc* overexpression can induce genomic DNA damage and compromise p53 function, presumably through a reactive oxygen species (ROS)-mediated mechanism (Vafa et al., 2002). Following γ radiation, *myc*-overexpressing cells are less efficient in G1 arrest compared to normal cells (Sheen and Dickson, 2002; Vafa et al., 2002), indicating that *myc*-overexpression could drive cells to progress through cell cycle in the presence of genomic DNA damage.

Based on recent discoveries from c-*myc* studies and our own results, we propose a model for the role of *mPer2* in tumor suppression (Figure 8). In this model, the loss of *mPer2* function results in dampened *Bmal1* expression and decreased intracellular levels of BMAL1/NPAS2 or BMAL1/CLOCK heterodimers, leading to the derepression of c-*myc* throughout 24 hr L/D cycles. Overexpression of c-*myc* causes genomic DNA damage and eventually leads to hyperplasia and tumor development. Following γ radiation, the loss of *mPer2* function partially impairs p53-mediated apoptosis, leading to accumulation of damaged cells. However, the *mPer2*$^{m/m}$ cells, expressing c-*myc* at elevated levels, could still progress through cell cycle in the presence of genomic DNA damage, resulting in the high incidence of tumor development after γ radiation.

In summary, loss of *mPer2* function results in increased tumor development and deficiencies in DNA damage responses in mice. Thus, the circadian clock not only organizes various biological processes, including cell proliferation, to allow an organism to adapt to the cyclic changes in the environment, but also plays an important role in the response to unpredicted hazards that are detrimental to genomic material. The circadian regulator mPER2, therefore, can be regarded as a tumor suppressor. The other circadian regulators may play a similar role in tumor suppression as well, since the core circadian genes show a coordinated regulation in vivo. It has been shown that the *Period2* gene also plays a critical role in circadian control in humans. Mutations in *hPer2* result in familial advanced sleep phase syndrome (Toh et al., 2001). It would be important to examine whether mutations in circadian genes also contribute to cancer development in humans.

Experimental Procedures

Animal Maintenance

Wild-type, *mPer2*$^{-/-}$, and *mPer2*$^{m/m}$ mice of similar genetic background (129/C57BL6) were housed in standard animal maintenance facility at constant temperature (21°C–23°C), humidity (50%–70%), air-flow rate (15 exchanges/hr); and 12 hr:12 hr L/D cycles (light on at ZT0 and off at ZT12).

γ Irradiation

Mice were irradiated at selected ZT times with a single dose of 4 Gy (16.8 cGy/sec) in a cesium-137 Gammacell. Cultured thymocytes were irradiated in culture flasks with the same dose.

Histological Analysis

Mice were killed by cervical dislocation. Tissue and tumor specimens were fixed in formalin. Paraffin sections were prepared and stained with haematoxylin and eosin. All tumor diagnoses were confirmed by histological examination.

Flow Cytometry

Mice were sacrificed at selected ZT times. Thymocytes were isolated from unirradiated and irradiated mice and fixed in 70% ethanol. After being incubated with PBS containing 50 μg/ml propidium io-

dide, 0.2% Tween 20, and 1 mg/ml RNase at 4°C overnight, samples were analyzed by a Becton Dickinson FACScan flow cytometer using CellQuest software (Becton Dickinson).

Northern Blot Analysis

Total RNA was isolated from mouse livers following standard procedure (Chirgwin et al., 1979). Twenty micrograms of total RNA was separated by electrophoresis and transferred onto a nylon membrane. The blots were hybridized with ^{32}P-labeled cDNA probes, washed, and exposed to X-ray film. The *mPer1, mPer2, Clock*, and *Cry1* probes have been described previously (Albrecht et al., 1997; Sun et al., 1997); the *Bmal1* probe was the 241–1172 nt fragment of *Bmal1* cDNA obtained from RT-PCR using a 5′ primer gaaagaggc gtcgggac and a 3′ primer acttgcctgtgacattgtgcgagg; the *Gapdh* probe was the Pst I fragment of rat *Gapdh* cDNA (Fort et al., 1985); the *Mdm*-2 probe was the Xho I fragment of MDM C14-2 plasmid (Oliner et al., 1992); the *Gadd45*α probe was the Sac I-Sac II fragment of pGEM-gadd45 plasmid; the *Cyclin D1* probe was the Eco RI-Hind III fragment of pD103 plasmid; the *Cyclin A* probe was the Eco RI fragment of pCycA plasmid; the *p53* probe was the Eco RI-Hind III fragment of pMO53 plasmid; the c-*myc* probe was the Xba I-Eco RI fragment of pCMV-*cMyc* plasmid; and the *Cdk-4* probe was the Hind III-Not I fragment of pRC/CMV-CDK4 plasmid (Matsushime et al., 1991).

Western Blot Analysis

Thymocytes were isolated from wild-type and *mPer2*$^{m/m}$ mice and incubated in RPMI 1640 medium containing 15% fetal calf serum at 37°C for 2 hr before being treated with 4 Gy of γ radiation. Cell extracts for p53 study and mitochondria extracts for cytochrome c study were prepared as previously described (Fu and Benchimol, 1997; Gao et al., 2001). The extracts were separated by electrophoresis and transferred onto a nitrocellulose membrane. The levels of p53 and cytochrome c were detected using a p53-specific antibody PAb421 (Banks et al., 1986) and a mouse cytochrome c-specific antibody (Santa Cruz Biotechnology). The bound antibodies were detected using ECL reagents (Amersham). The blots were reprobed with a β-actin-specific antibody (Sigma) to provide a loading control.

Transient Transfection

The embryonic fibroblasts (MEFs) were isolated from *mPer2*$^{m/m}$ embryos at day E13.5 following standard procedures (Robertson, 1987). At 24 hr before transfection, cells of passage 2 were plated in 6-well plates with a density of 2.5×10^5 cells per well. Cells were then transfected by LipofectAmine (GIBCO-BRL) following standard procedure. A total amount of 1.2 μg DNA was used for each transfection, which contained an invariant of 20 ng or 40 ng dose of Luciferase reporter plasmid along with varying amounts of expression vectors for *Npas2, Bmal1, Cry1* (Reick et al., 2001), and *mPer2* (Albrecht et al., 1997), and the empty vector pcDNA3 (Invitrogene). Cell extracts were prepared at 24 hr after transfection. The protein concentration in cell extracts was determined by Bio-Rad protein assay (Bradford, 1976). Luciferase activity in 20 μg of cell extracts was measured using a TD-20/201 luminometer (Turner Designs).

Acknowledgments

We thank Dr. L. Donehower for providing the pGEM-gadd45 plasmid; Dr. K. Galaktionov for providing the pD103 and pCycA plasmids; Dr. S. McKnight for providing the expression vectors encoding NPAS2, BMAL1, and CRY1; Dr. L. Penn for providing the XNM-Luc and SNM-Luc plasmids; Dr. H. Okamura for providing the mPer1-Luc plasmid; Dr. X. Wu for providing the pCMV-cMyc plasmid and the PAb421 and 2A10 antibodies; Drs. J. Ma and C. Struckenholz for helping analyze the data; Ms. K. Nolan for preparing histological slides; Ms. L. Feng for flow cytometry analysis; and Drs. L. Donehower, S. Benchimol, M. Patel, and P. Hastings for helpful discussions. This work is supported by grants from the National Institute of Health and Clayton Foundation for Research.

Received: February 14, 2002
Revised: August 9, 2002

References

Albrecht, U., Sun, Z.S., Eichele, G., and Lee, C.C. (1997). A differential response of two putative mammalian circadian regulators, mPer1 and mPer2 to light. Cell *91*, 1055–1064.

Anderson, L.E., Morris, J.E., Sasser, L.B., and Stevens, R.G. (2000). Effect of constant light on DMBA mammary tumorigenesis in rats. Cancer Lett. *148*, 121–126.

Bae, K., Jin, X., Maywood, E.S., Hastings, M.H., Reppert, S.M., and Weaver, D.R. (2001). Differential functions of *mPer1*, *mPer2*, and *mPer3* in the SCN circadian clock. Neuron *30*, 525–536.

Balsalobre, A., Damiola, F., and Schibler, U. (1998). A serum shock induces circadian gene expression in mammalian tissue culture cells. Cell *93*, 929–937.

Banks, L., Matlashewski, G., and Crawford, L. (1986). Isolation of human p53-specific monoclonal antibodies and their use in the studies of human p53 expression. Eur. J. Biochem. *159*, 529–534.

Barbason, H., Herens, C., Robaye, B., Milis, G., Sulon, J., Bouzahzah, B., and VanCantfort, J. (1995). Importance of cell kinetics rhythmicity for control of cell proliferation and carcinogenesis in rat liver. In Vivo *9*, 539–548.

Battey, J., Moulding, C., Taub, R., Murphy, W., Stewart, T., Potter, H., Lenoir, G., and Leder, P. (1983). The human c-myc oncogene: structural consequences of translocation into the IgH locus in Burkitt lymphoma. Cell *34*, 779–787.

Bjarnason, G.A., and Jordan, R. (2000). Circadian variation of cell proliferation and cell cycle protein expression in man: clinical implications. Prog. Cell Cycle Res. *4*, 193–206.

Bjarnason, G.A., Jordan, R.C., and Sothern, R.B. (1999). Circadian variation in the expression of cell-cycle proteins in human oral epithelium. Am. J. Pathol. *154*, 613–622.

Blackwell, T.K., Huang, J., Ma, A., Kretzner, L., Alt, F.W., Eisenman, R.N., and Weintraub, H. (1993). Binding of myc proteins to canonical and noncanonical DNA sequences. Mol. Cell. Biol. *13*, 5216–5224.

Bradford, M.M. (1976). A rapid and sensitive method for the quantitation of microgram quantities of protein utilizing the principle of protein-dye binding. Anal. Biochem. *72*, 248–258.

Chirgwin, J.M., Przybyla, A.E., MacDonald, R.J., and Rutter, W.J. (1979). Isolation of biologically active ribonucleic acid from sources enriched in ribonuclease. Biochemistry *18*, 5294–5299.

Clarke, A.R., Purdie, C.A., Harrison, D.J., Morris, R.G., Bird, C.C., Hooper, M.L., and Wyllie, A.H. (1993). Thymocyte apoptosis induced by p53-dependent and independent pathways. Nature *362*, 849–852.

Evan, G.I., and Vousden, K.H. (2001). Proliferation, cell cycle and apoptosis in cancer. Nature *411*, 342–348.

Facchini, L.M., Chen, S., Marhin, W.W., Lear, J.N., and Penn, L.Z. (1997). The myc negative auto regulation mechanism requires Myc-Max association and involves the c-*Myc* p2 minimal promoter. Mol. Cell. Biol. *17*, 100–114.

Fort, P., Marty, L., Piechaczyk, M., Sabrouty, S.E., Dani, C., Jeanteur, P., and Blanchard, J.M. (1985). Various rat adult tissues express only one major mRNA species from the glyceraldehyde-3-phosphate-dehydrogenase multigenic family. Nucleic Acids Res. *13*, 1431–1442.

Fu, L., and Benchimol, S. (1997). Participation of the human p53 3′UTR in translational repression and activation following gamma-irradiation. EMBO J. *16*, 4117–4125.

Gao, C.F., Ren, S., Zhang, L., Nakajima, T., Ichinose, S., Hara, T., Koike, K., and Tsuchida, N. (2001). Caspase-dependent cytosolic release of cytochrome c and membrane translocation of Bax in p53-induced apoptosis. Exp. Cell Res. *265*, 145–151.

Giaccia, A.J., and Kastan, M.B. (1998). The complexity of p53 modulation: emerging patterns from divergent signals. Genes Dev. *12*, 2973–2983.

Green, D.R., and Reed, J.C. (1998). Mitochondria and apoptosis. Science *281*, 1309–1312.

Hansen, J. (2001). Increased breast cancer risk among women who work predominantly at night. Epidemiology *12*, 74–77.

Hecht, J.L., and Aster, J.C. (2000). Molecular biology of Burkitt's lymphoma. J. Clin. Oncol. *18*, 3707–3721.

Hrushesky, W.J. (2001). Tumor chronobiology. J. Controlled Release *74*, 27–30.

Klevecz, R.R., Shymko, R.M., Blumenfeld, D., and Braly, P.S. (1987). Circadian gating of S phase in human ovarian cancer. Cancer Res. *47*, 6267–6271.

Kornmann, B., Preitner, N., Rifat, D., Fleuury-Olela, F., and Schibler, U. (2001). Analysis of circadian liver gene expression by ADDER, a highly sensitive method for the display of differentially expressed mRNAs. Nucleic Acids Res. *29*, E51.

Lee, T.C., and Ziff, E.B. (1999). Mxi1 is a repressor of the c-myc promoter and reverses activation by USF. J. Biol. Chem. *274*, 595–606.

Lowe, S.W., Schmitt, E.M., Smith, S.W., Osborne, B.A., and Jacks, T. (1993). p53 is required for radiation-induced apoptosis in mouse thymocytes. Nature *362*, 847–849.

Matsushime, H., Roussel, M.F., Ashmun, R.A., and Sherr, C.J. (1991). Colony-stimulating factor 1 regulates novel cyclins during the G1 phase of the cell cycle. Cell *65*, 701–713.

McNamara, P., Seo, S., Daniel, R., Sehgal, A., Chakravarti, D., and FitzGerald, G.A. (2001). Regulation of CLOCK and MOP4 by nuclear hormone receptors in the vasculature: a humoral mechanism to reset a peripheral clock. Cell *105*, 877–889.

Oliner, J.D., Kinzler, K.W., Meltzer, P.S., George, D.L., and Vogelstein, B. (1992). Amplification of a gene encoding a p53-associated protein in human sarcomas. Nature *358*, 80–83.

Panda, S., Antoch, M.P., Miller, B.H., Su, A.I., Schook, A.B., Straume, M., Schultz, P.G., Kay, S.A., Takahashi, J.S., and Hogenesch, J.B. (2002). Coordinated transcription of key pathways in the mouse by the circadian clock. Cell *109*, 307–320.

Pelengaris, S., Khan, M., and Evan, G.I. (2002). Suppression of Myc-induced apoptosis in beta cells exposes multiple oncogenic properties of Myc and triggers carcinogenic progress. Cell *109*, 321–334.

Pucci, B., Kasten, M., and Giordano, A. (2000). Cell cycle and apoptosis. Neoplasia. *2*, 291–299.

Reick, M., Garcia, J.A., Dudley, C., and McKnight, S.L. (2001). NPAS2: an analog of CLOCK operative in the mammalian forebrain. Science *293*, 506–509.

Reppert, S.M., and Weaver, D.R. (2001). Molecular analysis of mammalian circadian rhythms. Annu. Rev. Physiol. *63*, 647–676.

Robertson, E.J. (1987). Embryo-derived stem cell lines. In Teratocarcinomas and Embryonic Stem Cells: A Practical Approach. J. Robertson, ed. (Oxford: IRL Press), pp. 71–112.

Ruifrok, A.C.C., Weil, M.M., Thames, H.D., and Mason, K.A. (1998). Diurnal variations in the expression of radiation-induced apoptosis. Radiat. Res. *149*, 360–365.

Rutter, J., Reick, M., Wu, L.C., and McKnight, S.L. (2001). Regulation of Clock and NPAS2 DNA binding by the redox state of NAD cofactors. Science *293*, 510–514.

Shearman, L.P., Sriram, S., Weaver, D.R., Maywood, E.S., Chaves, I., Zheng, B., Kume, K., Lee, C.C., van der Horst, G.T., Hastings, M.H., and Reppert, S.M. (2000). Interacting molecular loops in the mammalian circadian clock. Science *288*, 1013–1019.

Sheen, J.H., and Dickson, R.B. (2002). Overexpression of c-Myc alters G(1)/S arrest following ionizing radiation. Mol. Cell. Biol. *22*, 1819–1833.

Sherr, C.J. (1996). Cancer cell cycles. Science *274*, 1672–1677.

Spencer, C.A., and Groudine, M. (1991). Control of c-myc regulation in normal and neoplastic cells. Adv. Cancer Res. *56*, 1–48.

Sun, Z.S., Albrecht, U., Zhuchenko, O., Bailey, J., Eichele, G., and Lee, C.C. (1997). RIGUI, a putative mammalian ortholog of the *Drosophila* period gene. Cell *90*, 1003–1011.

Toh, K.L., Jones, C.R., He, Y., Eide, E.J., Hinz, W.A., Virshup, D.M., Ptacek, L.J., and Fu, Y.H. (2001). An hPer2 phosphorylation site mutation in familial advanced sleep phase syndrome. Science *291*, 1040–1043.

Vafa, O., Wade, M., Kern, S., Beeche, M., Pandita, T.K., Hampton, G.M., and Wahl, G.M. (2002). c-Myc can induce DNA damage, increase reactive oxygen species, and mitigate p53 function. A mechanism for ontogeny-induced genetic instability. Mol. Cell *9*, 1031–1044.

Vogelstein, B., Lane, D., and Levine, A.J. (2000). Surfing the p53 network. Nature *408*, 307–310.

Winningham, M.L. (2001). Strategies for managing cancer-related fatigue syndrome: a rehabilitation approach. Cancer *92* (*suppl 4*), 988–997.

Wood, P.A., Hrushesky, W.J., and Klevecz, R. (1998). Distinct circadian time structures characterize myeloid and erythroid progenitor and multipotential cell clonogenicity as well as marrow precursor proliferation dynamics. Exp. Hematol. *26*, 523–533.

Yamaguchi, S., Mitsui, S., Miyake, S., Yan, L., Onishi, H., Yagita, K., Suzuki, M., Shibata, S., Kobayashi, M., and Okamura, H. (2000). The *5′* upstream region of *mPer1* gene contains two promoters and is responsible for circadian oscillation. Curr. Biol. *10*, 873–876.

You, Z., Saims, D., Chen, S., Zhang, Z., Guttridge, D.C., Guan, K.L., MacDougald, O.A., Brown, A.M., Evan, G., Kitajewski, J., and Wang, C.Y. (2002). Wnt signaling promotes oncogenic transformation by inhibiting c-Myc-induced apoptosis. J. Cell Biol. *157*, 429–440.

Young, M.W., and Kay, S.A. (2001). Time zones: a comparative genetics of circadian clocks. Nat. Rev. Genet. *2*, 702–715.

Zheng, B., Larkin, D.W., Albrecht, U., Sun, Z.S., Sage, M., Eichele, G., Lee, C.C., and Bradeley, A. (1999). The mPer2 gene encodes a functional component of the mammalian circadian clock. Nature *400*, 169–173.

Zheng, B., Albrecht, U., Kaasik, K., Sage, M., Lu, W., Vaishnav, S., Li, Q., Sun, Z.S., Eichele, G., Bradley, A., and Lee, C.C. (2001). Nonredundant roles of the mPer1 and *mPer2* genes in the mammalian circadian clock. Cell *105*, 683–694.

Zylka, M.J., Shearman, L.P., Weaver, D.R., and Reppert, S.M. (1998). Three period homologs in mammals: differential light responses in the suprachiasmatic circadian clock and oscillating transcripts outside of brain. Neuron *20*, 1103–1110.